Comparison between Monomeric and Polymeric Surfactants .1. Micellar Solution of the Monomer

ARTICLE *in* THE JOURNAL OF PHYSICAL CHEMISTRY · APRIL 1992

Impact Factor: 2.78 · DOI: 10.1021/j100188a057

4 AUTHORS, INCLUDING:

Walter Richtering
RWTH Aachen University
237 PUBLICATIONS **6,048** CITATIONS
SEE PROFILE

Walther Burchard
University of Freiburg
141 PUBLICATIONS **3,116** CITATIONS
SEE PROFILE

Comparison between Monomeric and Polymeric Surfactants. 1. Micellar Solution of the Monomer

Rolf Löffler, Walter H. Richtering, Heino Finkelmann, and Walther Burchard*

Institut für Makromolekulare Chemie, Universität Freiburg, Stefan-Meier Strasse 31, D-7800 Freiburg, Germany *(Received: October 25, 1991; In Final Form: January 2, 1992)*

We have synthesized a new nonionic surfactant with the chemical formula $CH_2{=}C(CH_3)COO(CH_2)_{11}(OCH_2CH_2)_8OCH_3$. This amphiphilic molecule contains the polymerizable methacrylate group at the end of the hydrophobic moiety, which permits preparation of polymeric nonionic surfactants. Isotropic aqueous solutions have been investigated by static and dynamic light scattering and viscometry in a broad concentration and temperature range. Phase separation on heating with a lower critical solution temperature of 43 °C and a hexagonal liquid crystalline phase were observed. In dilute solution spherical micelles with an aggregation number of 70 and a radius of 3.4 nm were found at low temperatures. At higher temperatures the molar mass increases, which can be explained by an aggregation of spherical micelles to random clusters. In semidilute solution the concentration dependence of the reduced osmotic modulus $(M_w/RT)(\partial\pi/\partial c)$ is close to the theoretical behavior of hard spheres, and good agreement with the $C_{14}E_8$ surfactant is found. An increase of correlation length was observed at concentrations close to the hexagonal mesophase, indicating a formation of an ordered structure. By measurements of the depolarized scattering intensity the hexagonal to isotropic phase transition could be detected. In contrast to the isotropic to nematic phase transition of thermotropic liquid crystals, no orientation fluctuations were observed within the isotropic region in the vicinity of the lyotropic-phase transition.

1. Introduction

In aqueous solution amphiphilic molecules aggregate to micelles above a critical micelle concentration. Such solutions have been the object of research for many years, with special interest in shape and size of these micellar aggregates.[1-3] Different structures are known: spherical, wormlike, or disklike micelles. Size and shape depend strongly on the molecular structure of the amphiphilic molecule, which can be divided into ionic surfactants, where strong Coulombic interactions are present, and nonionic surfactants. An often studied group of nonionic surfactants is the poly(ethylene glycol) monoalkyl ether of the general structure $C_mH_{2m+1}(OCH_2CH_2)_nOH$ (C_mE_n). In aqueous solutions of C_mE_n surfactants, two interesting features are observed. (i) Isotropic micellar solutions undergo phase separation on heating. Such behavior is typical of hydrophobic interaction and is also observed with several water-soluble polymers. Hydrophobic interaction results from a change of order in the water structure, related to attractive interactions of a hydrophobic segment with water molecules.[4,5] (ii) At high concentration liquid crystalline (LC) phase behavior is observed with several different structures.[6]

Phase diagrams of many C_mE_n systems are known and demonstrate the complex influence of hydrophilic-hydrophobic balance on miscibility gap and mesophases.[7] There is much discussion of the micelle structure within the isotropic solution involving different models like anisotropic growth[8-10] or statistical association of micelles.[1,11-13] Unambiguous description of the solution structure is difficult because size and shape of micellar aggregates can change with temperature and concentration.

In this study a nonionic surfactant with a slightly different structure has been investigated:

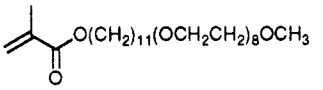

At the end of the *hydrophobic* moiety a methacrylate group is introduced, which allows polymerization. At the *hydrophilic* end a methoxy group replaces the hydroxy group; in the following discussion this surfactant will be called $MC_{11}E_8$. Although the length of $MC_{11}E_8$ in the all-trans configuration (5.4 nm) is nearly the same as that of the $C_{14}E_8$ surfactant,[13] different solution behavior is expected due to changes in the hydrophilic-hydrophobic balance. The $MC_{11}E_8$ surfactant has been studied for two reasons. First, influences of the chemical structure on solution properties can be obtained from comparison between different low molar mass amphiphilic substances. Second, solutions of this monomeric surfactant can be used as a reference state for the polymeric surfactant.

In this contribution static and dynamic light scattering and viscosity measurements from dilute and semidilute solutions of $MC_{11}E_8$ in water are discussed and will be compared with results from C_mE_n surfactants. In a second paper properties of aqueous and nonaqueous solutions of the corresponding polysurfactants will be reported.[14]

2. Experimental Section

The synthesis of $MC_{11}E_8$ is described in detail in ref 15. The monomer was purified by flash chromatography[16] (Kieselgel 60, Merck) using a 1:1 mixture of ether and acetone ($r_f = 0.51$). The solvent was removed under vacuum at 0 °C. Analytical HPLC showed that the monomer was pure. The monomer was stored at −20 °C with 100 ppm 2,4-di-*tert*-butylcresol as inhibitor. Spectroscopic characterization: (a) by 1330 Perkin-Elmer infrared spectrometer, IR (film) 1705 (C=O), 1620 (C=C), 1100 cm^{-1}

(1) Degiorgio, V. In *Physics of Amphiphiles: Micelles, Vesicles and Microemulsions*; Degiorgio, V., Corti, M., Eds. North-Holland: Amsterdam, 1985.
(2) *Surfactants in Solution*; Mittal, K. L., Bothorel, P., Eds.; Plenum Press: New York, 1986; Vols. 4-6.
(3) *Surfactant Science Series*; Schick, M. J., Ed.; M. Dekker: New York, 1987; Vol. 23.
(4) Franks, F. In *Water: A Comprehensive Treatise*; Franks, F., Ed.; Plenum Press: New York, 1975; Vol. 4.
(5) Tanford, C. *The Hydrophobic Effect*; Wiley: New York, 1973.
(6) Tiddy, G. J. T.; Walsh, M. F. *Stud. Phys. Theor. Chem.* **1983**, *26*, 151.
(7) Mitchell, D. J.; Tiddy, G. J. T.; Warring, L.; Bostock, T.; McDonald, M. P. *J. Chem. Soc., Faraday Trans. 1* **1983**, *79*, 975.
(8) Ravey, J. C. *J. Colloid Interface Sci.* **1983**, *94*, 289.
(9) Cebula, D. J.; Ottewill, R. H. *Colloid Polym. Sci.* **1982**, *260*, 1182.
(10) Brown, W.; Johnsen, R.; Stilbs, P.; Lindman, B. *J. Phys. Chem.* **1983**, *87*, 4548.
(11) Zulauf, M.; Rosenbusch, J. P. *J. Phys. Chem.* **1983**, *87*, 856.
(12) Zulauf, M.; Weckström, K.; Hayter, J. B.; Degiorgio, V.; Corti, M. *J. Phys. Chem.* **1985**, *89*, 3411.
(13) Richtering, W. H.; Burchard, W.; Jahns, E.; Finkelmann, H. *J. Phys. Chem.* **1988**, *92*, 6032.
(14) Richtering, W. H.; Löffler, R.; Burchard, W. *Macromolecules*, in press.
(15) Löffler, R. Ph.D. Thesis, Freiburg, 1990. Löffler, R.; Finkelmann, H., manuscript in preparation.
(16) Still, W. C.; Kahn, M.; Mitra, A. *J. Org. Chem.* **1978**, *43*, 2923.

0022-3654/92/2096-3883$03.00/0

(C—O). (b) Bruker WP80 CW spectrometer ^{1}H NMR ($DCCl_3$/TMS) δ 1.3 (m, 18 H, $CH_2CH_2CH_2$), 1.9 (s, 3 H, $H_2C{=}C(CH_3)COO$), 3.4 (s, 3 H, OCH_3), 3.7 (m, 36 H, CH_2O), 4.1 (t, 2 H, $COOCH_2$), 5.5 (m, 1 H, $HCH{=}C(CH_3)$, cis), 6.1 ppm (s, 1 H, $HCH{=}C(CH_3)$, trans).

The determination of the phase diagram was performed with a Leitz Ortholux II Pol BK microscope, equipped with a Mettler FP80/FP82 hot stage. Both static and dynamic light scattering were measured simultaneously with an automatic ALV goniometer and an ALV Structurator/Correlator ALV 3000. An argon ion laser was used as the light source (λ_0 = 496.5 nm). A high-quality Glan-Thomson prism (Bernhard Halle Nachfolger, Berlin) was used for measurements of depolarized scattering intensity. The alignment was checked by measuring the depolarization ratio of toluene. Solutions were prepared by filtration through Millipore filters (0.22 μm). The refractive index increment was measured with a Brice Phoenix differential refractometer and was found to be

$$dn/dc = 0.144 - [0.0004(T - 10)]$$

where dn/dc is in cm^3/g and T is in °C. Viscosity measurements had been performed with a Haake Rotovisco RV 100 instrument using a couette system according to Mooney–Edward (shear rate 0–60 s^{-1}) and an Ubbelhode viscosimeter. Solutions had been filtered (0.45 μm) before measurements. Temperature accuracy was ±0.1 °C.

3. Theoretical Background

Static light scattering from solutions is commonly described by Debye's equation[17-20]

$$\frac{Kc}{R(\theta)} = \frac{1}{P'(\theta)} \frac{1}{RT} \frac{\partial \pi}{\partial c} \tag{1}$$

Here K is an optical contrast factor which depends sensitively on the refractive index increment dn/dc. $R(\theta) = i(\theta)r^2/I$ is the Rayleigh ratio, where $i(\theta)$ and I are the scattering intensity at scattering angle θ and the primary beam intensity, respectively, and r is the distance of the detector from the scattering center. $P'(\theta) = i(\theta)/i(\theta{=}0)$ is an apparent scattering factor which gives information on the particle's shape and the structure of the solution. In general $P'(\theta)$ for isotropic systems is given by

$$P'(\theta) = \frac{1}{n^2} \sum_i^n \sum_j^n \left\langle \frac{\sin (\mathbf{r}_{ij} \cdot \mathbf{q})}{\mathbf{r}_{ij} \cdot \mathbf{q}} \right\rangle \tag{2}$$

where $\mathbf{r}_{ij}$ is the distance between two scattering centers i and j. The magnitude of the scattering vector $\mathbf{q}$ is

$$|\mathbf{q}| = (4\pi/\lambda) \sin (\theta/2) \tag{3}$$

where λ is the wavelength of the light in the solution. The brackets $\langle\ \rangle$ in eq 2 indicate the ensemble average over all possible distances occurring between the two scattering centers i and j. In some cases $P'(q)$ can be factorized as[20]

$$P'(q) = P(q)S(q)/S(0) \tag{4}$$

where the particle scattering factor $P(q)$ arises from the individual particle whereas the structure factor $S(q)$ reflects the arrangement of the centers of mass of the various particles in space. Equation 4 is exact only for hard spheres, but it can be used as a fairly good approximation for general structures.

At zero scattering angle, light scattering is only determined by a thermodynamic quantity, the inverse osmotic compressibility (i.e., osmotic modulus)

$$\frac{Kc}{R(\theta{=}0)} = \frac{1}{RT} \frac{\partial \pi}{\partial c} = \frac{1}{M_{app}} \tag{5}$$

For low concentrations a virial expansion can be made which yields

$$\frac{Kc}{R(\theta{=}0)} = \frac{1}{M_w}(1 + 2A_2M_wc + 3A_3M_wc^2 + ...) \tag{6}$$

By extrapolation to zero angle, the weight-average molar mass M_w and second virial coefficient A_2 are obtained. From A_2 an equivalent thermodynamic hard-sphere radius R_{eq} can be calculated by use of the well-known formula for hard spheres:[21]

$$A_2 = 4N_AV_m/M^2 \quad \text{with} \quad V_m = (4\pi/3)R_{eq}^3 \tag{7}$$

In dynamic light scattering a time correlation function is measured, and from the first cumulant Γ, the mutual diffusion coefficient is obtained.[22]

$$\lim_{q^2 \to 0} (\Gamma/q^2) = D_c \tag{8}$$

Irreversible thermodynamics show that the concentration dependence of D_c is given by[21]

$$D_c = (k_BT/f_c)[(M_w/RT)(\partial \pi/\partial c)] = (k_BT/f_c)[M_wKc/R_{\theta=0}] \tag{9}$$

where k_B is Boltzmann's constant and f_c is the concentration-dependent friction coefficient. In dilute solution the concentration dependence can often be described by the linear equation

$$D_c = D_z^0(1 + k_Dc) \tag{10}$$

From the diffusion coefficient at infinite dilution D_z^0, a hydrodynamic radius R_h is calculated from the Stokes–Einstein law.

The viscosity of solutions of spherical particles is described by Einstein's equation[23]

$$\eta = \eta_0(1 + 2.5\phi) \tag{11}$$

where η_0 is the solvent viscosity and ϕ is the volume fraction of the solute. A general equation for the reduced viscosity was given by Huggins[24]

$$\eta_{red} = [\eta] + k[\eta]^2c \tag{12}$$

with

$$\eta_{red} = \frac{\eta - \eta_0}{\eta_0 c} \qquad \lim_{\substack{c \to 0 \\ \dot{\gamma} \to 0}} \eta_{red} = [\eta] \tag{13}$$

Here $[\eta]$ is the intrinsic viscosity obtained from extrapolation of η_{red} to zero concentration and zero shear rate. The Huggins constant depends on the particle's structure; a value of 2.0 was calculated for hard spheres.[25,26] With eq 11 a hydrodynamic radius can be determined from $[\eta]$. The volume fraction ϕ is given by

$$\phi = \frac{N_AcV_{h\eta}}{M_w} \qquad r_{h\eta} = \left[\frac{3[\eta]M_w}{10\pi N_A} \right]^{1/3} \tag{14}$$

4. Results

The phase diagram of the binary system $MC_{11}E_8$/water is shown in Figure 1. At −8 °C and about 67% by weight of the amphiphile, a eutectic point is located. At temperatures above −8 °C to the water-rich side of the phase diagram from the eutectic point, two two-phase regions were observed, the hexagonal phase H_1 coexisting with ice (H_1 + ice) and the isotropic solution L_1 coexisting with ice (L_1 + ice). At the amphiphile-rich side, a two-phase region consisting of the hexagonal phase H_1 and crystalline amphiphile CA (H_1 + CA) and a two-phase region

(17) Debye, P. *Phys. Colloid Chem.* **1947**, *51*, 18.
(18) Albrecht, A. C. *J. Chem. Phys.* **1957**, *27*, 1014.
(19) Flory, P. J.; Bueche, A. M. *J. Polym. Sci.* **1958**, *27*, 219.
(20) Debye, P. *Ann. Phys.* **1915**, *46*, 809.
(21) Yamakawa, H. *Modern Theory of Polymer Solutions*; Harper & Row: New York, 1971.
(22) Berne, B. J.; Pecora, R. *Dynamic Light Scattering*; Wiley: New York, 1976.
(23) Einstein, A. *Ann. Phys.* **1911**, *34*, 598.
(24) Huggins, M. L.; Riseman, J. *J. Am. Chem. Soc.* **1942**, *64*, 2716.
(25) Tanford, C. *Physical Chemistry of Macromolecules*, Wiley: New York, 1961.
(26) Frisch, H. L.; Simha, R. In *Rheology*; Eirich, F. R., Ed.; Academic Press: New York, 1956; Vol. 1.

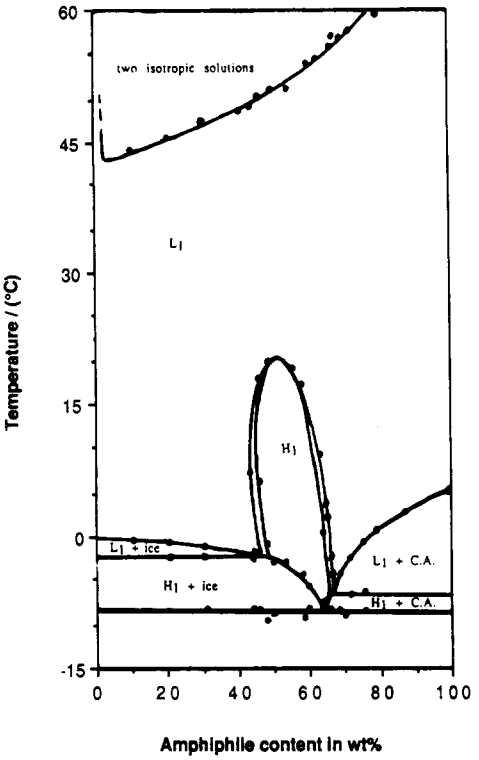

Figure 1. Phase diagram of $MC_{11}E_8$ in water.

TABLE I: Results from Light Scattering of Aqueous Solutions of $MC_{11}E_8$

T, °C	M_w, g/mol	10^4A_2, mol·cm³/g²	R_{eq}, nm	$10^7D_z^0$, cm²/s	R_h, nm	k_D, cm³/g
10	42400	2.3	3.4	4.81	3.3	3.0
15	45000	2.05	3.4	5.50	3.4	2.8
20	44900	1.74	3.3	6.30	3.4	2.1
30	59000	0.8	3.0	7.43	3.7	−0.8
35	96000	≈0.2	*a*	6.54	4.8	<0
40	500000	≈0.2	*a*	3.4	10.4	<0

[a] Not calculated due to the small magnitude of A_2.

TABLE II: Results from Viscosity Measurements of Aqueous Solutions of $MC_{11}E_8$

T, °C	$[\eta]$, cm³/g	k	R_h, nm	$R_{h\eta}$, nm
20	4.8	1.8	3.4	3.3
40	5.0	5.3	10.4	7.4

consisting of isotropic solution L_1 and crystalline amphiphile (L_1 + CA) was found. In the concentration range from 47% by weight of the amphiphile to 68% and in the temperature range from −8 to 20.5 °C, the hexagonal phase H_1 was located. Above 43 °C (lower critical consolution point) a miscibility gap was found where two isotropic solutions coexist.

Results of static and dynamic light scattering from dilute solutions are summarized in Table I. The molar mass measured at low temperatures corresponds to an aggregation number of 70. The dependence of the reduced viscosity on the concentration $c' = c - \text{cmc}$ is shown in Figure 2, where the critical micelle concentration is cmc = 3.4×10^{-4} mol/L.[15] The data obtained from extrapolation to infinite dilution are given in Table II. The effect of temperature on η_{red} at finite concentration is shown in Figure 3. Newtonian flow behavior was found at all concentrations.

Two series of light scattering measurements were performed at concentrations of 44% and 50%, respectively, which are close to the hexagonal liquid crystalline phase. The measurements of the first series were made completely within the isotropic region, but the distance from the hexagonal phase is very close at 15 °C and larger at 20 and 10 °C. The second series was carried out at the concentration of the LC-phase maximum, and the phase boundary was approached by changing the temperature between

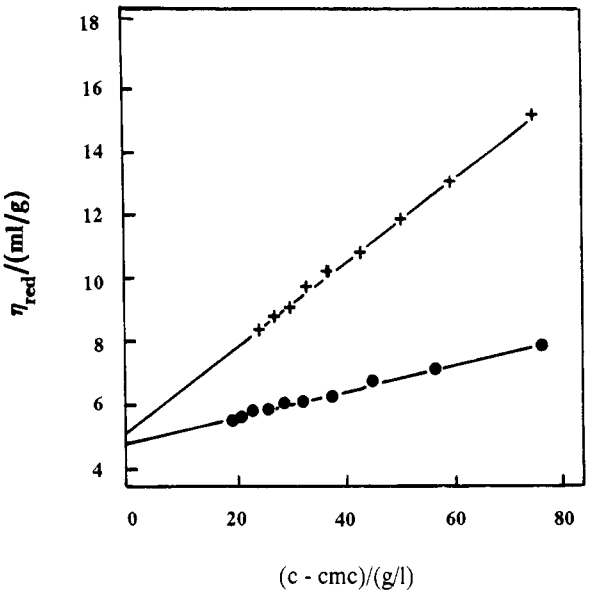

Figure 2. Concentration dependence of the reduced viscosity at 20 (●) and 40 °C (+).

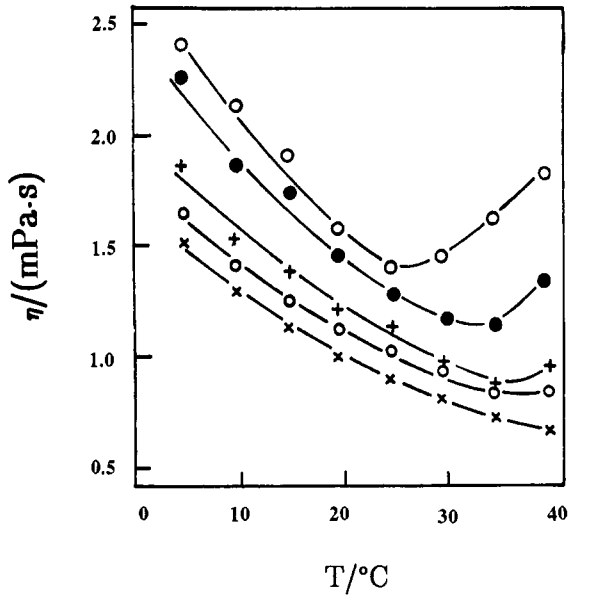

Figure 3. Temperature dependence of viscosity of $MC_{11}E_8$ in water. Key: pure water (×), 2.5% (○), 5% (+), 7.5% (●), 10% (○) (from below).

40 and 21 °C (the phase transition occurs at 20.5 °C).

The angular dependences of the scattered light at c = 44% (w/v) at 20, 15, and 10 °C are shown in Figure 4, parts a–c, respectively. At 20 and 10 °C a small-angle excess scattering was found, an observation which is well-known from semidilute polymer solutions. It indicates the presence of large particles.[27-29] At 15 °C a minimum was observed at $q \approx 1.1 \times 10^{-5}$ cm^{-1}, which corresponds to a maximum in the scattering intensity. This minimum was unexpected but was found reproducible in repeated measurements. In the second series at 50% (w/v), we expected critical behavior when approaching the phase maximum. Orientational fluctuations appeared conceivable, which would indicate a pretransitional LC behavior. Such orientational fluctuations are accompanied by depolarization, and for this reason, polarized and depolarized scattering intensities were recorded. Zimm plots from the polarized vv component at the three temperatures of 40, 30, and 21 °C are shown in Figure 5a–c, revealing again a strong influence

(27) Koberstein, J. T.; Picot, C.; Benoit, H. *Polymer* **1985**, *28*, 673.
(28) Huber, K.; Bantle, S.; Burchard, W.; Fetters, L. J. *Macromolecules* **1986**, *19*, 1404.
(29) Burchard, W. *Makromol. Chem. Macromol. Symp.* **1988**, *18*, 1.

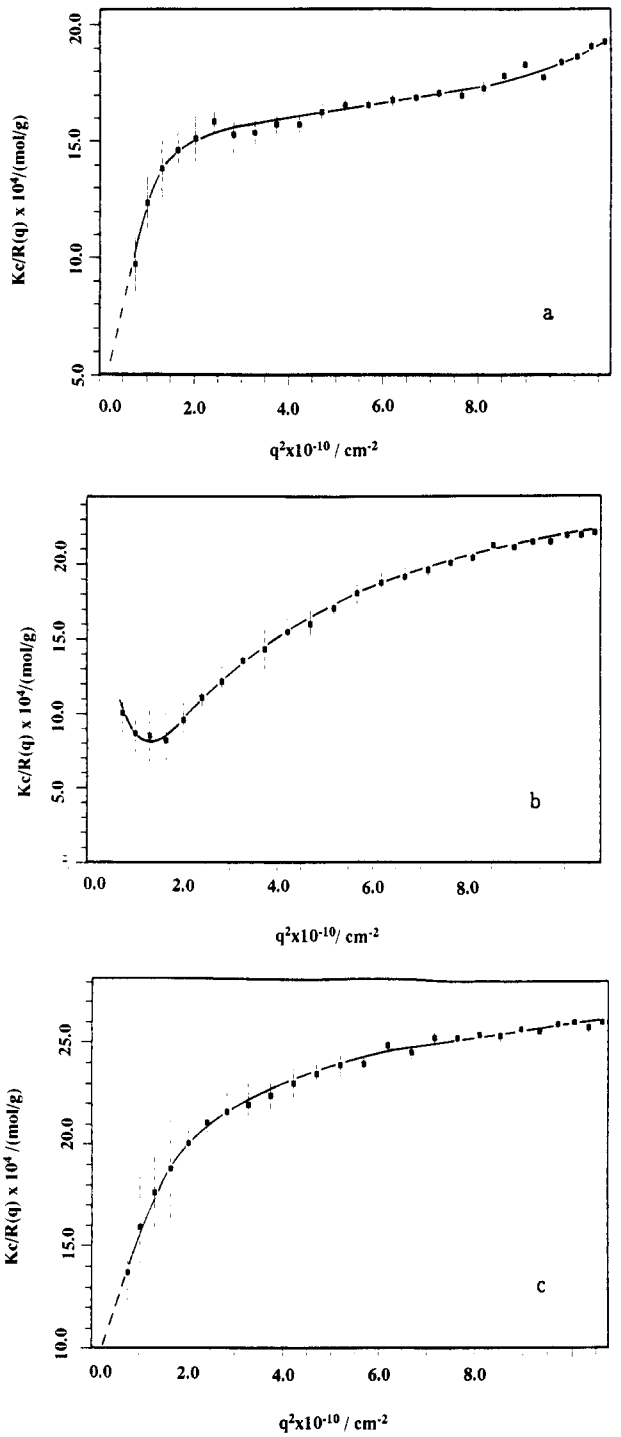

Figure 4. Angular dependence of static LS of $MC_{11}E_8$ at c = 44% at 20 (a), 15 (b), and 10 °C (c).

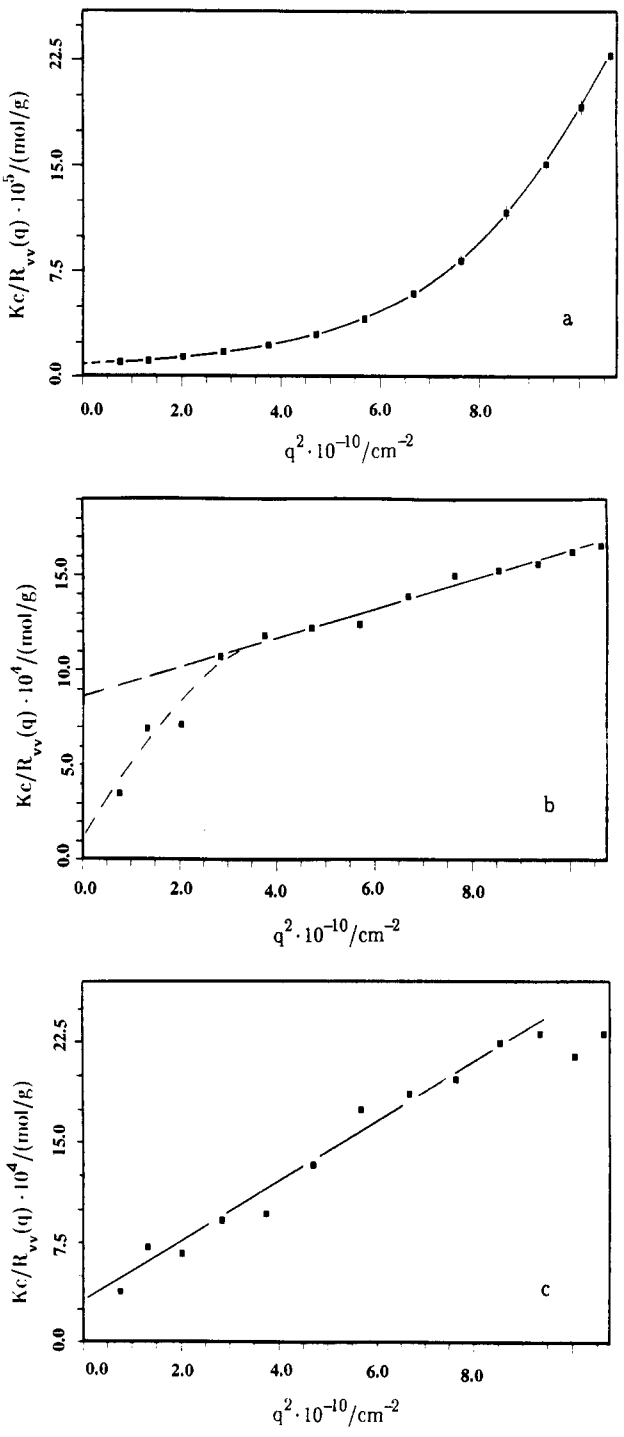

Figure 5. Angular dependence of static LS of $MC_{11}E_8$ at c = 50% at 40 (a), 30 (b), and 21 °C (c).

of temperature. At 40 °C the angular dependence follows the apparent particle scattering factor of spheres. The corresponding Guinier plot (not shown) gave a straight line over the whole accessible q-range. An apparent radius of gyration of 100 nm was found at 40 °C. Compared to the lower concentrations of the first series, a smaller $Kc/R_{\theta=0}$ value, i.e., larger apparent molecular weight, was measured. At 30 °C a low-angle excess scattering occurred, which was similar to that found with the solution of 44% at temperatures of 20 and 10 °C. An apparent radius of 50 nm was estimated from the low scattering angle region. At 21 °C the angular dependence became linear and the apparent radius of gyration was with 170 nm, again larger than at 30° and even larger than at 40 °C.

In a third series, the depolarized scattering was recorded at 50% in the temperature interval of 18–30 °C passing the boundary of the hexagonal phase. Measurements were performed at angles between 60 and 120°; no angular dependence was observed. The temperature was varied in the following manner: first the solution was held at 18 °C for 12 h, and then the depolarized scattering intensity was measured at different temperatures, with 30 °C being the highest temperature. Afterward the solution was cooled down again, and the scattering intensities were measured at the same temperatures as before. At each temperature the light scattering measurements were started after an equilibration time of 15 min. The results are shown in Figure 6.

5. Discussion

The comparison of the *phase diagrams* of $MC_{11}E_8$/water and $C_{14}E_8$/water[30] reveals two distinct differences. (i) The lower critical solution temperature (LCST) of $MC_{11}E_8$ is 26 K lower

(30) Jahns, E.; Finkelmann, H. *Colloid Polym. Sci.* **1987**, *265*, 304.

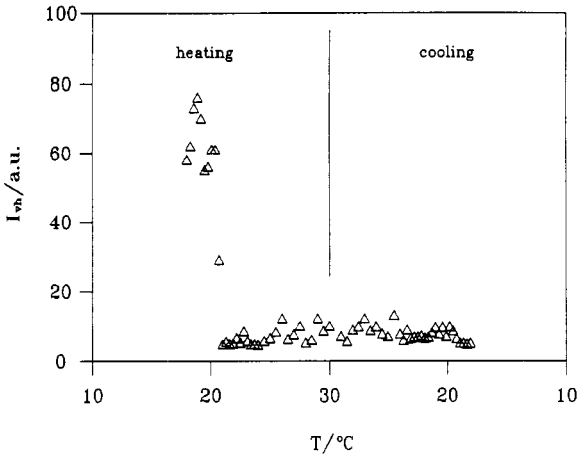

Figure 6. Temperature dependence of depolarized scattering intensity of $MC_{11}E_8$ at c = 50%.

than the LCST of the $C_{14}E_8$ surfactant in water. This observation indicates that methylation of the free alcohol group of common poly(ethylene glycol) monoalkyl ethers prevents the formation of additional hydrogen bonds with water molecules. The result agrees with a recently reported study by Conroy et al. on the influence of the terminal methoxy group on the phase behavior of nonionic surfactants.[31] (ii) Only one liquid crystalline phase was observed with $MC_{11}E_8$ instead of five different phases, which were observed in the case of $C_{14}E_8$. The occurrence of only one mesophase H_1 with a low maximum melting temperature can be related to a disturbed balance between the hydrophilic and the hydrophobic part of the $MC_{11}E_8$ molecule. The phase behavior resembles that of poly(ethylene glycol) monoalkyl ethers with a short alkyl chain,[7] indicating that the hydrophilic ester group is located at the hydrophilic–hydrophobic interface of the micelle.

Results of static and dynamic light scattering and viscometry on *dilute solutions* reveal a behavior which is rather common for nonionic surfactants. At low temperatures (≤20 °C), small spherical micelles are found. R_{eq}, the equivalent thermodynamic hard-sphere radius, agrees very well with the hydrodynamic radius determined by quasielastic light scattering and viscometry, and the values are close to that of the $C_{14}E_8$ micelle.[13] The aggregation number of 70 is much smaller than in the case of $C_{14}E_8$, but is close to that of poly(ethylene glycol) monoalkyl ethers with a short alkyl chain,[1] also indicating that the hydrophilic ester group is located at the hydrophilic–hydrophobic interface of the micelle. The observation that the $MC_{11}E_8$ and the $C_{14}E_8$ micelles have different aggregation numbers but the same radius illustrates the complex influence of the chemical structure of the amphiphilic molecule on the micellar structure.

At 20 °C a Huggins constant of 1.8 is found, which agrees with spherical micelles. In the theoretical equations on viscometry mentioned above, solvation of particles was not considered, but it is known that micelles are strongly hydrated.[32-34] From the different values of the intrinsic viscosity obtained from theory (2.5) and experiment (4.8), the excess volume due to bound water molecules can be determined. A value of 2390 water molecules per micelle was calculated, which corresponds to an average of 4.1 water molecules bound to one ethylene oxide group. This result is in good agreement with reported data from NMR measurements.[33,34]

At higher temperatures the solution behavior becomes more complicated. In light scattering an increase in the extrapolated molecular weight and hydrodynamic radius and a decrease of A_2 is observed. The viscosity at finite concentration also increases on heating, but nearly the same intrinsic viscosity was observed

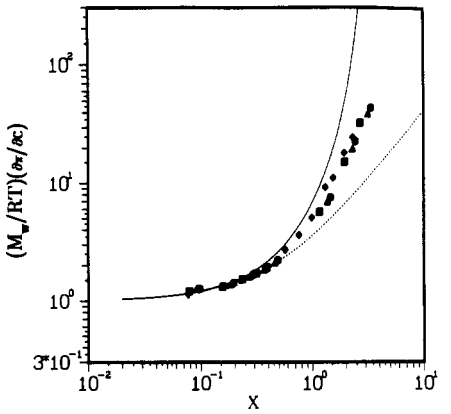

Figure 7. Plot of the reduced osmotic modulus vs the parameter $X = A_2M_wc$ of $MC_{11}E_8$ at 10 (●), 15 (▲), and 20 °C (■) and $C_{14}E_8$ at 25 °C (◆); hard spheres (—), flexible chains (···).

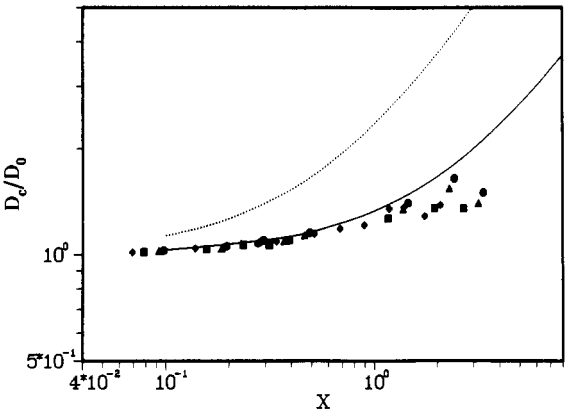

Figure 8. Plot of the reduced diffusion coefficient vs the parameter $X = A_2M_wc$ of $MC_{11}E_8$ at 10 (●), 15 (▲), and 20 °C (■) and $C_{14}E_8$ at 20 °C (◆); hard spheres (—),[40] flexible chains (···).[41]

at 20 and 40 °C, meaning the same hydrodynamic behavior at infinite dilution. The high molar mass is incompatible with a single spherical micelle and can be caused by either an anisotropic growth of spherical micelles to wormlike micelles or an association of spherical micelles to random clusters. Anisotropic micelles, however, should produce a significantly higher $[\eta]$, and deviations from Newtonian flow behavior are expected. The increase of η_{red} at finite concentration with increasing temperature is a consequence of an increase in hydrodynamic volume due to aggregation, which can also be seen from the higher Huggins constant k at 40 °C. Therefore the experimental data obtained from $MC_{11}E_8$ solutions support the model of aggregating micelles and hence support results obtained from the $C_{14}E_8$ surfactant[13] and studies by Zulauf et al.[12] and Matsumoto and Zenkoh[35] on different systems.

In *semidilute* solution, behavior similar to that of $C_{14}E_8$ was observed. The osmotic modulus is obtained from static light scattering at zero angle (eq 5). It is well-known that the reduced osmotic modulus $(M_w/RT)(\partial\pi/\partial c)$ can be expressed as a function of the dimensionless parameter $X = A_2M_wc$, which is proportional to c/c^*, where c^* is the overlap concentration.[36-38] Theoretical equations for the concentration dependence of the osmotic modulus of hard spheres (Carnahan–Starling equation[39]) and linear flexible-chain molecules (renormalization group theory[36]) are known and describe experimental data very well. Macromolecules of different architecture, for example, branched or rigid rodlike

(31) Conroy, J. P.; Hall, C.; Leng, C. A.; Rendall, K.; Tiddy, G. J. T.; Walsh, J.; Lindblom, G. *Prog. Colloid Polym. Sci.* **1990**, *82*, 253.
(32) Tanford, C.; Nozaki, Y.; Rhode, M. *J. Phys. Chem.* **1977**, *81*, 1555.
(33) Nilsson, P. G.; Lindman, B. *J. Phys. Chem.* **1983**, *87*, 4756.
(34) Carlström, G.; Halle, B. *J. Chem. Soc., Faraday Trans. 1* **1989**, *85*, 1049.
(35) Matsumoto, T.; Zenkoh, H. *Colloid Polym. Sci.* **1990**, *268*, 536.
(36) Ohta, T.; Oono, Y. *Phys. Lett. A.* **1982**, *89A*, 460.
(37) Wiltzius, P.; Haller, H. R.; Cannell, D. S.; Schaefer, D. W. *Phys. Rev. Lett.* **1983**, *51*, 1183.
(38) Freed, K. *Renormalization Group Theory of Macromolecules*; Wiley: New York, 1987.
(39) Carnahan, N. F.; Starling, K. E. *J. Chem. Phys.* **1969**, *51*, 635.

molecules, obey characteristic deviations from the behavior of flexible polymers and hard spheres, respectively.[29] That means that the concentration dependence of the osmotic modulus permits the determination of the architecture of the particles in concentrated solution. In Figure 7 measurements from $MC_{11}E_8$ at low temperatures are plotted together with theoretical curves for hard spheres and flexible-chain molecules. Good agreement with $C_{14}E_8$ data was found, indicating that spherical micelles exist even at high concentrations. The concentration dependence of the reduced diffusion coefficient also shows good agreement for both surfactants (Figure 8).

At even *higher concentrations* the scattered intensity becomes angle dependent, Figures 4 and 5. With the 44% solution a small-angle excess scattering was observed at 10 and 20 °C, a feature that has also been observed in polymer solutions and the $C_{14}E_8$ surfactant. The appearance of excess scattering means that the solution is no longer homogeneous, but large particles are formed,[27,29] in this case, clusters of small micelles. The angular dependence in Figure 4a,c can be extrapolated to zero scattering angle by extrapolating measurements at either small or large angles, respectively. From the extrapolation of the measurements at large angles, the osmotic modulus inside the large cluster is obtained and these data are plotted in Figure 6; the concentration dependence shows that the large clusters are built by spherical micelles. Extrapolation of the measurements at small scattering angle yields the apparent molar mass of the clusters and leads to a drop off of the osmotic modulus curve.

At c = 44% and 15 °C, a peak is observed in the scattering function which is caused by a structured solution.[42] As already mentioned, the angular dependence is described by $P'(\theta)$. In the case of hard spheres, $P'(\theta)$ can be separated into the particle form factor $P(\theta)$ (particle scattering) and the structure factor $S(\theta)$ (interparticle scattering). $P(\theta)$ can be measured at infinite dilution. In micellar solutions the situation is more complicated since the particle size and shape can change with concentration and a straightforward analysis of $P'(\theta)$ becomes difficult. However, from the position of the maximum in Figure 4b, the distance between the centers of mass of the large clusters can be roughly estimated to be 500 nm. The structure peak observed in light scattering should not be mistaken for the peak observed in neutron scattering. Light scattering is fully equivalent to neutron scattering but allows structure determination on a different length scale. In a recent neutron scattering study by Zulauf et al.,[12] micellar solutions of different nonionic surfactants were investigated. Small spherical micelles were found in the whole isotropic region. Combining the results from both techniques and taking into account that the length scale probed by neutron scattering is much shorter than that of light scattering, one can describe the structure of concentrated solutions with small spherical micelles that aggregate to clusters near the mesophase.

A second way of approaching the liquid crystalline phase is by changing the temperature. At 50% the hexagonal phase is stable up to 20.5 °C, and with changing temperature one can study the solution structure at different distances to the mesophase. Figure 5 reveals a strong influence of temperature on the scattered intensity. At 40 °C the large clusters are of spherical shape. The temperature dependence of the radius indicates that the clusters first dissociate on cooling, but close to the liquid crystalline phase they grow again. However, no form factor of spheres is observed at 21 °C.

If the scattering centers have an anisotropic polarizability and the primary beam is vertically polarized, then the scattered light contains a horizontally polarized component.[43,44] Hence anisotropic structures can be detected by measuring the depolarized component. It is known that close to the isotropic–nematic phase transition of thermotropic liquid crystals orientation fluctuations are observed which cause a divergence of polarized and depolarized scattering intensity at the phase transition.[45,46] Therefore the *depolarized* intensity I_{vh} (the first index denotes the polarization of the primary beam, the second that of the scattered light) was measured at c = 0.5 g/mL as a function of temperature. In the case of $MC_{11}E_8$ an interesting phenomenon was observed: the hexagonal phase is birefringent but not turbid. Therefore it was possible to measure I_{vh} even at temperatures below the phase transition at 20.5 °C. From Figure 6 two interesting features can be seen. (i) On *heating*, the depolarized intensity sharply decreases at the phase transition. Above the clearing temperature, I_{vh} is temperature independent and no orientation fluctuations are observed. (ii) On *cooling*, no increase of I_{vh} is observed at the phase transition. However, if the sample is stored at 18 °C, I_{vh} increases slowly after 7 h and finally reaches the same value that was observed in the beginning. Investigation of the phase transition by polarizing microscopy showed that the solution becomes birefringent immediately after the temperature is below 20.5 °C. Apparently depolarized light scattering detects the anisotropic phase only when the order expands over a longer length scale. The long lag time means that the formation of large-scale liquid crystalline order is very slow, probably due to a high viscosity in the hexagonal phase.

6. Conclusions

Micellar solutions of the nonionic surfactant $MC_{11}E_8$ were studied by light scattering and viscometry, and interesting behavior was observed. The different chemical structure of $MC_{11}E_8$ compared to common poly(ethylene glycol) monoalkyl ethers affects the phase behavior and the micellar structure. The occurrence of only one lyotropic liquid crystalline phase and the small aggregation number resemble the properties of C_mE_n surfactants with short alkyl chains. These observations indicate that the ester group is located at the hydrophobic–hydrophilic interface of the micelle.

At low temperatures small spherical micelles are formed which aggregate to random clusters with increasing temperature. No indications for a transition from spherical to anisotropic micelles were found.

At high concentrations near the hexagonal phase, large particles were observed. The formation of long-range structures formed by small micelles may indicate pretransitional effects. However, no orientation fluctuations were observed within the isotropic region, although the hexagonal to isotropic phase transition can be detected by depolarized light scattering.

Acknowledgment. We are greatly indebted to the Deutsche Forschungsgemeinschaft (Sonderforschungsbereich 60) for financial support. We thank T. Koch for his support of the time-consuming measurements of depolarized scattering intensity and J. Arroyo and I. Kühn for technical assistance. W.H.R. thanks the Graduiertenkolleg Polymerwissenschaften for a scholarship.

Registry No. $MC_{11}E_8$, 129522-76-5.

(40) Batchelor, G. K. *J. Fluid Mech.* **1976**, *52*, 245.
(41) Oono, Y.; Baldwin, P. R.; Ohta, T. *Phys. Rev. Lett.* **1984**, *53*, 2149.
(42) Guinier, A.; Fournet, G. *Small Angle Scattering of X-Rays*; Wiley: New York, 1955.
(43) Gans, R. *Ann. Phys.* **1912**, *37*, 881.
(44) Horn, P.; Benoit, H. *J. Polym. Sci.* **1953**, *10*, 29.
(45) De Gennes, P.-G. *Mol. Cryst. Liq. Cryst.* **1971**, *12*, 193.
(46) Zink, M.; de Jeu, W. *Mol. Cryst. Liq. Cryst.* **1985**, *124*, 287.